

On the generation of shelves by long nonlinear waves in stratified flows

By DILIP PRASAD AND T. R. AKYLAS

Department of Mechanical Engineering, Massachusetts Institute of Technology,
Cambridge, MA 02139, USA

(Received 31 January 1997 and in revised form 1 May 1997)

The phenomenon of shelf generation by long nonlinear internal waves in stratified flows is investigated. The problem of primary interest is the case of a uniformly stratified Boussinesq fluid of finite depth. In analysing the transient evolution of a finite-amplitude long-wave disturbance, the expansion procedure of Grimshaw & Yi (1991) breaks down far downstream, and it proves expedient to follow a matched-asymptotics procedure: the main disturbance is governed by the nonlinear theory of Grimshaw & Yi (1991) in the ‘inner’ region, while the ‘outer’ region comprises multiple small-amplitude fronts, or shelves, that propagate downstream and carry $O(1)$ mass. This picture is consistent with numerical simulations of uniformly stratified flow past an obstacle (Lamb 1994). The case of weakly nonlinear long waves in a fluid layer with general stratification is also examined, where it is found that shelves of fourth order in wave amplitude are generated. Moreover, these shelves may extend both upstream and downstream in general, and could thus lead to an upstream influence of a type that has not been previously considered. In all cases, transience of the main nonlinear wave disturbance is a necessary condition for the formation of shelves.

1. Introduction

The theory of waveguides provides a useful model for a variety of wave phenomena in geophysical fluid dynamics such as the propagation of internal waves in the oceanic thermocline. In these problems, nonlinear effects are of particular interest owing to the possibility of permanent wave disturbances which remain coherent over large distances and times. While there is an extensive body of prior work on nonlinear internal waves in stratified fluids, one aspect that appears to have escaped attention is the formation of shelves by nonlinear transient disturbances. It is precisely this aspect that we explore in some detail here. Shelves are small-amplitude streamwise structures of large extent and have been encountered before in studies of solitary-wave propagation in slowly varying media (Leibovich & Randall 1973; Johnson 1973; Newell 1985). However, as will be seen, the mechanism by which shelves are formed in the present context is somewhat different.

In a stratified fluid layer of finite depth, the Korteweg–de Vries (KdV) equation is central to the propagation of long internal waves with small, but not infinitesimal, amplitude. The KdV equation combines the leading-order nonlinear and dispersive effects for each long-wave mode and admits solitary-wave solutions with a ‘sech²’ profile. While it is possible to obtain higher-order approximations as indicated by Benney (1966), the validity of this weakly nonlinear–weakly dispersive approach is limited to small-amplitude disturbances. In the special case of a uniformly stratified

(constant Brunt–Väisälä frequency) Boussinesq fluid, however, it so happens that a linear long-wave mode is also a solution of the full nonlinear equations of motion, and it becomes feasible to set up a nonlinear theory. Using a novel approach pioneered by Warn (1983), Grimshaw & Yi (1991, referred to hereinafter as GY) showed that the appropriate evolution equation, that replaces the KdV equation in this anomalous case, is of the integral–differential type and describes long waves of finite amplitude as long as no breaking streamlines are present in the flow field.

The flow configuration examined by GY is the main focus of the present investigation. In discussing the transient development of a finite-amplitude long-wave mode, it becomes apparent that the asymptotic theory of GY breaks down far downstream of the main disturbance owing to the formation of an infinite shelf; moreover, mass is not conserved. These difficulties are handled by following a matched-asymptotics procedure: the nonlinear theory of GY is valid in an ‘inner’ region, while the downstream flow defines an ‘outer’ region governed by the linear hydrostatic equations of motion. The shelf is seen to have a large but finite extent and its structure is obtained by matching these two regions, thereby satisfying mass conservation. The asymptotic results are supported by the numerical work of Lamb (1994) which contains evidence for shelf formation in uniformly stratified flow past an obstacle.

The possibility of shelf generation in a fluid layer with general stratification is then examined in the weakly nonlinear–weakly dispersive régime. It is found that the shelf amplitude is considerably smaller than in the fully nonlinear case. It is noteworthy, however, that here shelves can propagate upstream of the main wave disturbance, a feature that bears on the question of upstream influence in nonlinear stratified flow over topography.

2. Review of long-wave theory

Consider the classical problem of internal-wave propagation in an inviscid incompressible stratified fluid layer of depth h . Taking L to denote the horizontal lengthscale of the disturbance and N_0 a characteristic value of the Brunt–Väisälä frequency, we have the following dimensionless parameters:

$$\mu = \frac{h}{L}, \quad \beta = \frac{N_0^2 h}{g},$$

g being the gravitational acceleration. The parameter μ controls dispersive effects and is key to the development of a long-wave theory, while the Boussinesq parameter β provides a measure of stratification.

We shall use dimensionless variables throughout, scaling the horizontal coordinate x with L , the vertical coordinate y with h and time t with $L/(h N_0)$. The density of the undisturbed fluid is $\bar{\rho}(y)$ and the Brunt–Väisälä frequency $N(y)$ is defined by the relation

$$\beta \bar{\rho} N^2 = -\bar{\rho}_y. \quad (2.1)$$

For two-dimensional disturbances (independent of the spanwise direction), it is convenient to introduce the streamfunction Ψ such that the horizontal and vertical velocity components, respectively, are given by $u = \Psi_y$ and $v = -\Psi_x$; thus incompressibility is automatically satisfied. The remaining governing equations of mass conservation and momentum balance, after eliminating the pressure, may then be cast in the form

$$\rho_t + J(\rho, \Psi) = 0, \quad (2.2)$$

$$(\rho \Psi_{yt})_y + [\rho J(\Psi_y, \Psi)]_y - \frac{1}{\beta} \rho_x = -\mu^2 \{[\rho J(\Psi_x, \Psi)]_x + (\rho \Psi_{xt})_x\}, \quad (2.3)$$

where ρ is the fluid density and $J(a, b)$ stands for the Jacobian $a_x b_y - a_y b_x$. Furthermore, assuming the fluid layer to be bounded above and below by rigid walls, the appropriate boundary conditions are

$$\Psi_x = 0 \quad (y = 0, 1). \quad (2.4)$$

The significance of the parameter μ is brought out more clearly by considering the propagation of infinitesimal long waves. Upon linearizing equations (2.2) and (2.3), Ψ and ρ satisfy, to leading order in μ , the linear hydrostatic equations

$$\rho_t + \beta \bar{\rho} N^2 \Psi_x = 0, \quad (2.5)$$

$$\beta (\bar{\rho} \Psi_{yt})_y - \rho_x = O(\mu^2). \quad (2.6)$$

Equations (2.5) and (2.6), subject to the boundary conditions (2.4), admit separable solutions of the form

$$\Psi = A(x \pm ct) \phi(y), \quad \rho - \bar{\rho} = \mp \frac{\beta}{c} \bar{\rho} N^2 \Psi. \quad (2.7)$$

The wave-amplitude profile A propagates with constant speed c which is determined, along with the corresponding vertical mode shape $\phi(y)$, from the eigenvalue problem

$$(\bar{\rho} \phi_y)_y + \frac{\bar{\rho} N^2}{c^2} \phi = 0 \quad (0 \leq y \leq 1), \quad (2.8a)$$

$$\phi = 0 \quad (y = 0, 1); \quad (2.8b)$$

in general, there is an infinite number of eigensolutions $\{\phi_n(y), c_n\}$ ($n = 1, 2, \dots$) which form an orthogonal and complete set. Hence, dispersive effects are completely absent in the long-wave limit $\mu \rightarrow 0$, and one can trace the transient development of a general initial disturbance using superposition of the long-wave modes (2.7).

Improving on the linear hydrostatic approximation, the classical theoretical approach uses perturbation expansions to derive evolution equations for the amplitude $A(x, t)$ of a long-wave mode, taking into account weak nonlinear and dispersive effects. Specifically, A satisfies the KdV equation to leading order, and one may obtain higher-order amplitude equations following a systematic expansion procedure (Benney 1966).

The present study is motivated by the fact that, as will be seen, long-wave expansions become non-uniform in the far field of a transient nonlinear disturbance in a stratified fluid layer. Physically, these non-uniformities reveal the formation of streamwise structures of large extent, termed shelves, that are essential in satisfying mass conservation. The phenomenon of shelf generation, although it has a counterpart in the weakly nonlinear-weakly dispersive régime (see §7), is most significant for disturbances of finite amplitude. Accordingly, we shall first concentrate on the case of a uniformly stratified Boussinesq fluid for which, as pointed out by GY, it is feasible to set up a finite-amplitude long-wave theory. Moreover, there exist detailed numerical simulations of this type of stratified flow past an obstacle, allowing comparison against the analytical predictions (see §6).

In preparation for discussing the mechanism of shelf generation, we now review the essentials of the theory of GY. In the special case of uniform Boussinesq stratification ($N = 1, \beta \rightarrow 0$), the eigenvalue problem (2.8) can be solved in closed form:

$$\phi_n(y) = \sin \frac{y}{c_n}, \quad c_n = \frac{1}{n\pi} \quad (n = 1, 2, \dots). \quad (2.9)$$

Furthermore, these background flow conditions imply that Long's model is applicable, so the governing equations for steady nonlinear flow reduce to a linear form (Long 1953). As a result, each linear long-wave mode (2.7) also satisfies the nonlinear governing equations (2.2) and (2.3) (in the hydrostatic limit $\mu \rightarrow 0$), and this forms the basis of the nonlinear theory of GY.

Concentrating then on a finite-amplitude long-wave disturbance of mode n , say, that moves from right to left, the goal is to derive an evolution equation for the wave-amplitude profile A , taking into account weak dispersive effects ($\mu \ll 1$). To this end, it is convenient to adopt a reference frame moving with speed $-c_n$ (or, equivalently, to superimpose a uniform stream c_n); the disturbance is then expected to evolve on the slow timescale $T = \mu^2 t$ in this reference frame owing to the $O(\mu^2)$ dispersive corrections on the right-hand side of (2.3). Moreover, from (2.2), the density ρ is conserved along streamlines to leading order in μ . Hence, provided no breaking streamlines (implying overturning) are present, the vertical coordinate y may be replaced by Ψ and, upon integration along a streamline, (2.2) yields

$$\rho = \bar{\rho} \left(\frac{\Psi}{c_n} \right) - \mu^2 \bar{\rho}_\Psi \int_{-\infty}^x dx' \frac{\Psi_T}{\Psi_y} \Big|_\Psi, \quad (2.10)$$

where the subscript $|\Psi$ indicates that Ψ is held constant.

Using (2.10), the momentum equation (2.3) may then be manipulated to the form

$$\Psi_{yy} + \frac{\Psi - c_n y}{c_n^2} = -\mu^2 (\Psi_{xx} + R), \quad (2.11)$$

where

$$c_n R = y \frac{\partial}{\partial \Psi} \int_{-\infty}^x dx' \frac{\Psi_T}{\Psi_y} \Big|_\Psi - \frac{\partial}{\partial \Psi} \int_{-\infty}^x dx' y \frac{\Psi_T}{\Psi_y} \Big|_\Psi + c_n \frac{\partial}{\partial \Psi} \int_{-\infty}^x dx' \Psi_{yT} \Big|_\Psi. \quad (2.12)$$

Following a multiple-scale perturbation procedure, the streamfunction Ψ is now expanded according to

$$\Psi = \Psi^{(0)} + \mu^2 \Psi^{(1)} + \dots, \quad (2.13)$$

and using (2.11) along with the boundary conditions (2.4), we find that

$$\Psi^{(0)} = c_n y + A(x, T) \sin n\pi y, \quad (2.14)$$

the amplitude $A(x, T)$ being as yet undetermined.

At the next order in μ^2 , $\Psi^{(1)}$ satisfies

$$\Psi_{yy}^{(1)} + \frac{\Psi^{(1)}}{c_n^2} = -\Psi_{xx}^{(0)} - R^{(0)}, \quad (2.15)$$

subject to the homogeneous boundary conditions (2.4), where $R^{(0)} = R(x, \Psi^{(0)}, T)$. Invoking the standard orthogonality argument – for this inhomogeneous problem to have a solution the right-hand side of (2.15) has to be orthogonal to the corresponding homogeneous solution $\sin n\pi y$ – then leads to the desired evolution equation for $A(x, T)$:

$$K(x, x) A_T + \int_{-\infty}^x dx' \frac{\partial}{\partial x} K(x, x') A'_T - \frac{1}{2} c_n^3 A_{xxx} = 0, \quad (2.16)$$

where primed variables are functions of the integration variable x' . The kernel $K(x, x')$

is defined by

$$K(x, x') = c_n \int_0^{c_n} d\Psi \, y_A [y'_A + c_n(y'y'_A)_\Psi - c_n y y'_A] , \tag{2.17}$$

where $y = y(\Psi; A)$ is determined by inverting the leading-order expression (2.14) for the streamfunction $\Psi = \Psi^{(0)} + O(\mu^2)$. This inversion is possible only as long as

$$|A| \leq c_n^2 ; \tag{2.18}$$

when the magnitude of A reaches the critical value of c_n^2 , the flow features vertical streamlines and hence (2.18) represents a criterion for incipient breaking.

In the small-amplitude limit, $|A| \ll c_n^2$, equation (2.14) can be inverted using power series in A to obtain an analytical expression for $y = y(\Psi; A)$, which when inserted into (2.17) yields the following small-amplitude expansion for the kernel:

$$K(x, x') = 1 - c_n^{-4} (\frac{3}{4} A'^2 - 2AA' + \frac{3}{4} A^2) + \dots ; \tag{2.19}$$

substituting (2.19) into (2.16) and making use of the fact that $A_T = \frac{1}{2} c_n^3 A_{xxx} + O(A^3)$ we then obtain, correct to $O(A^3)$,

$$A_T - \frac{1}{2} c_n^3 A_{xxx} + \frac{1}{4c_n} AA_x A_{xx} + \frac{1}{4c_n} A^2 A_{xxx} - \frac{1}{2c_n} (A_x)^3 = 0 . \tag{2.20}$$

As already remarked, for the background flow conditions assumed here, the equations governing steady disturbances can be cast into a linear form, consistent with the evolution equation (2.16) where nonlinearity derives from transience only. As a result, a quadratic KdV-like term AA_x does not appear in the weakly nonlinear version (2.20). Of course, such a term will show up if one allows for small deviations from uniformly stratified Boussinesq flow, as explained in GY.

3. Non-uniform behaviour far downstream

Taking the wave-amplitude profile to be locally confined at $T = 0$, $A(x, 0) \rightarrow 0$ ($x \rightarrow \pm\infty$), the evolution equation (2.16) ensures that $A(x, T)$, and hence the $O(1)$ disturbance in (2.14), remains locally confined for $T > 0$. It is important to note, however, that higher-order corrections to the flow field extend infinitely far downstream, implying that the long-wave expansion of GY becomes non-uniform there.

Specifically, the inhomogeneous equation (2.15) governing $\Psi^{(1)}$ reduces far downstream ($x \rightarrow \infty$) to

$$\Psi_{yy}^{(1)} + \frac{\Psi^{(1)}}{c_n^2} = -R_\infty^{(0)} . \tag{3.1}$$

But, from (2.12), the right-hand side $R_\infty^{(0)} = \lim_{x \rightarrow \infty} R^{(0)}$ is, in general, non-zero; consequently, $\Psi^{(1)}$ features a uniform downstream shelf:

$$\Psi^{(1)} \sim \Psi_\infty^{(1)}(y, T) \quad (x \rightarrow \infty) . \tag{3.2}$$

Furthermore, proceeding to higher order, one expects the $O(\mu^4)$ correction to the streamfunction to grow linearly with x far downstream, indicating that expansion (2.13) breaks down when $x = O(\mu^{-2})$. A similar non-uniformity was noted by Warn (1983) in his study of finite-amplitude Rossby waves.

Turning attention next to the downstream density perturbation, using (2.14), ex-

pression (2.10) in the limit $x \rightarrow \infty$ may be written, correct to $O(\mu^2)$, as

$$\rho_\infty - \bar{\rho}(y) = -\mu^2 \frac{\beta}{c_n} (\Psi_\infty^{(1)} + \eta_T), \quad (3.3)$$

where

$$\eta = \int_{-\infty}^{\infty} \delta(A', \Psi^{(0)}) dx',$$

$\delta = y - \Psi^{(0)}/c_n$ being the vertical streamline displacement associated with the $O(1)$ disturbance (since A is locally confined so is δ). Therefore, the density perturbation does not vanish far downstream owing to the permanent distortion of the streamlines, caused by $\Psi_\infty^{(1)}$, and to the transient evolution of the main disturbance. From (3.1) and (2.12), however, it is evident that the streamfunction shelf $\Psi_\infty^{(1)}$ is also brought about by transient effects, so transience is solely responsible for this non-uniform behaviour.

In particular, in the weakly nonlinear régime ($|A| \ll c_n^2$),

$$\delta \sim -\frac{A}{c_n} \sin \frac{\Psi}{c_n^2} + \frac{A^2}{2c_n^3} \sin \frac{2\Psi}{c_n^2} + \frac{A^3}{8c_n^5} \left(\sin \frac{\Psi}{c_n^2} - 3 \sin \frac{3\Psi}{c_n^2} \right) + \dots, \quad (3.4)$$

and, making use of (2.19) and (2.20), expression (3.3) for the density perturbation far downstream yields

$$c_n(\rho_\infty - \bar{\rho}) + \beta \mu^2 \Psi_\infty^{(1)} = \frac{\mu^2 \beta}{8c_n^5} (\sin n\pi y + 3 \sin 3n\pi y) \frac{d}{dT} \int_{-\infty}^{\infty} A^3 dx + O(A^5). \quad (3.5)$$

Finally, considering a control volume extending from $x = -\infty$ to $x = \infty$ and using (3.3), one finds that the net mass flux out of the main nonlinear wave is given by

$$\frac{dM}{dT} = -\beta \int_0^1 dy \eta_T, \quad (3.6)$$

from which it is evident that mass is not conserved in general.

The non-uniformities noted above in the downstream flow field and the fact that mass conservation appears to be violated are reminiscent of the difficulties encountered previously in studies of the propagation of solitary waves in water of slowly varying depth, described by the perturbed KdV equation (see, for example, Leibovich & Randall 1972; Johnson 1973). In that problem, the non-uniformities behind the main wave, where a shelf forms, can be handled by a matched-asymptotics procedure (Kodama & Ablowitz 1981; Newell 1985) which reveals that the shelf has finite extent. To satisfy mass conservation, however, one has to recognize the existence of a reflected wave which moves in the direction opposite to that of the solitary wave and is therefore not described by the perturbed KdV equation (Knickerbocker & Newell 1980; Newell 1985). In the present problem, as discussed below, the resolution of the difficulties is somewhat more complicated owing in part to the fact that a stratified fluid layer supports multiple modes in the vertical direction, unlike the surface-wave problem where no such structure exists.

4. Shelf dynamics

As noted above, the long-wave expansion of GY breaks down far downstream of the main disturbance when $x = O(\mu^{-2})$. This suggests introducing the rescaled streamwise coordinate $X = \mu^2 x$ that will be used in describing the downstream flow

field, following a matching procedure: the nonlinear theory of GY is valid in the ‘inner’ region $x = O(1)$ while in the ‘outer’ region $X = O(1)$, given that the main disturbance is locally confined, the development of shelves downstream is expected to be governed by the linearized equations of motion. The specification of the flow field is completed by matching the inner and outer flows in the intermediate region $1 \ll x \ll \mu^{-2}$. In carrying out this programme, we shall take the main disturbance to be of mode one ($n = 1$).

We begin by determining $\Psi_\infty^{(1)}$ from the inhomogeneous equation (3.1). Expanding $R_\infty^{(0)}$ in terms of the long-wave modes (2.9), the solution of (3.1) may be written as

$$\Psi_\infty^{(1)} = G_1 \sin \pi y + \sum_{m=2}^\infty \frac{G_m}{\pi^2(m^2 - 1)} \sin m\pi y, \tag{4.1}$$

where

$$G_m(T) = 2 \int_0^1 dy R_\infty^{(0)} \sin m\pi y \quad (m \geq 2).$$

We remark that even though $R_\infty^{(0)}$ is orthogonal to $\sin \pi y$ in view of the solvability condition imposed on (2.15), it is still necessary to add a mode-1 term to $\Psi_\infty^{(1)}$, the coefficient $G_1(T)$ being thus far undetermined. As will be seen, this term arises from the coupling of $\Psi_\infty^{(1)}$ to the downstream density perturbation $\rho_\infty - \bar{\rho}$.

Using (4.1) and decomposing η_T into long-wave modes, expression (3.3) for the downstream density perturbation then yields

$$\rho_\infty - \bar{\rho} = -\mu^2 \frac{\beta}{c_1} \left[(G_1 + P_1) \sin \pi y + \sum_{m=2}^\infty \left\{ \frac{G_m}{\pi^2(m^2 - 1)} + P_m \right\} \sin m\pi y \right], \tag{4.2}$$

where

$$P_m(T) = 2 \int_0^1 dy \eta_T \sin m\pi y \quad (m \geq 1).$$

Unlike $G_1(T)$, the coefficient $P_1(T)$ above is known in terms of the $O(1)$ flow. In fact, in the small-amplitude limit, using (2.20) and (3.4) it follows that

$$\int_0^1 dy \eta_T \sin \pi y = \frac{1}{16c_1^5} \frac{d}{dT} \int_{-\infty}^\infty A^3 dx + O(A^5)$$

from which it is clear that P_1 is non-zero in general.

We now turn our attention to the outer region, $X = O(1)$. Since the main disturbance is locally confined, the downstream flow perturbations are $O(\mu^2)$, and we may write the streamfunction and density in the outer region as

$$\Psi = c_1 y + \mu^2 \hat{\psi}(X, y, T), \quad \rho = \bar{\rho}(y) + \mu^2 \beta \hat{\rho}(X, y, T). \tag{4.3}$$

Hence, to leading order in μ , $\hat{\psi}$ and $\hat{\rho}$ are governed by the linear hydrostatic equations (2.5) and (2.6):

$$\begin{aligned} \hat{\rho}_T + c_1 \hat{\rho}_X &= -\hat{\psi}_X, & (4.4) \\ \hat{\psi}_{yyT} + c_1 \hat{\psi}_{yyX} &= \hat{\rho}_X. & (4.5) \end{aligned}$$

In addition, from the boundary conditions (2.4), $\hat{\psi}_X$ must vanish on $y = 0, 1$.

Motivated by expressions (4.1) and (4.2) obtained from the inner flow, the solution

to the outer equations (4.4) and (4.5) is posed as

$$\widehat{\psi} = \sum_{m=1}^{\infty} Q_m(X, T) \sin m\pi y, \quad (4.6a)$$

$$\widehat{\rho} = \sum_{m=1}^{\infty} S_m(X, T) \sin m\pi y. \quad (4.6b)$$

Thus, the boundary conditions on $y = 0, 1$ are automatically met and upon substitution of (4.6) into (4.4) and (4.5) it is found that for each $m \geq 1$

$$\left(\frac{\partial}{\partial T} + c_1 \frac{\partial}{\partial X} \right) S_m = -Q_{mX}, \quad (4.7)$$

$$\left(\frac{\partial}{\partial T} + c_m^+ \frac{\partial}{\partial X} \right) \left(\frac{\partial}{\partial T} + c_m^- \frac{\partial}{\partial X} \right) Q_m = 0, \quad (4.8a)$$

where

$$c_m^{\pm} = c_1 \pm c_m. \quad (4.8b)$$

Based on (4.6), (4.7) and (4.8), the downstream flow is expected to consist of pairs of linear long-wave modes, one moving at a speed c_m^+ and the other at a speed c_m^- relative to the main disturbance – since $c_1 > c_m$ ($m \geq 2$), $c_m^{\pm} > 0$ so all modes appear downstream ($X > 0$). This provides an explanation for the non-uniform behaviour, noted in §3, of the inner flow far downstream ($x \gg 1$): the mode-1 nonlinear wave, through a mechanism of transient self-interaction manifested in the kernel (2.17), generates higher-mode linear long waves which travel at their own speeds. Specifically, after a time t , the two wavefronts corresponding to the m th mode, say, will be located at $x = (c_1 \pm c_m)t$. However, since t is related to the ‘slow’ time T of the nonlinear theory by $t = T/\mu^2$, these fronts (shelves) stretch to $x = \infty$ in the limit $\mu \rightarrow 0$. The preceding discussion also indicates that the mode-1 ($m = 1$) contribution to the outer flow must be treated separately because the speed $c_1^- = 0$ is associated with the nonlinear disturbance.

The structure of the downstream flow is now obtained by matching the inner and outer expressions for the streamfunction and density perturbations in the region $1 \ll x \ll \mu^{-2}$ ($x \rightarrow \infty$, $X \rightarrow 0$). Specifically, from (3.2), (3.3) and (4.3), one has

$$\widehat{\psi}|_{X \rightarrow 0} = \Psi_{\infty}^{(1)}, \quad (4.9a)$$

$$\widehat{\rho}|_{X \rightarrow 0} = -\frac{1}{c_1} (\Psi_{\infty}^{(1)} + \eta_T). \quad (4.9b)$$

For $m \neq 1$, the general solution of (4.8a) is

$$Q_m(X, T) = Q_m^+(\xi_m^+) H(\xi_m^+) + Q_m^-(\xi_m^-) H(\xi_m^-) \quad (m \geq 2), \quad (4.10a)$$

where $H(x)$ is the Heaviside step function and the characteristics ξ_m^{\pm} are defined by

$$\xi_m^{\pm} = T - \frac{X}{c_m^{\pm}}.$$

Using (4.7), we then find that

$$S_m(X, T) = \frac{1}{c_m} \{ Q_m^+(\xi_m^+) H(\xi_m^+) - Q_m^-(\xi_m^-) H(\xi_m^-) \} \quad (m \geq 2). \quad (4.10b)$$

Employing the matching conditions (4.9) along with (4.1), (4.2) and (4.10) and solving the resulting linear system for $Q_m^\pm(T)$, one has

$$Q_m^\pm(T) = \frac{1}{2} \left\{ \frac{G_m(T)}{m\pi^2(m \pm 1)} \mp \frac{P_m(T)}{m} \right\} \quad (m \geq 2). \tag{4.11}$$

Turning attention now to the mode-1 contribution, (4.8a) yields for $m = 1$

$$\frac{\partial}{\partial T} \left(\frac{\partial}{\partial T} + 2c_1 \frac{\partial}{\partial X} \right) Q_1 = 0, \tag{4.12}$$

while the matching condition (4.9a) along with (4.1) require

$$Q_1(0, T) = G_1(T). \tag{4.13}$$

Solving (4.12) subject to the condition (4.13), we obtain

$$Q_1(X, T) = G_1 \left(T - \frac{X}{2c_1} \right) H \left(T - \frac{X}{2c_1} \right).$$

The unknown function G_1 is finally determined by imposing the matching condition (4.9b) for the density perturbation. Specifically, making use of (4.7) for $m = 1$ and from (4.1) and (4.2), one has

$$G_1 = -\frac{1}{2} P_1.$$

Hence, the streamwise structure of the mode-1 shelf is given by

$$Q_1(X, T) = -\frac{1}{2} P_1 \left(T - \frac{X}{2c_1} \right) H \left(T - \frac{X}{2c_1} \right), \tag{4.14a}$$

$$S_1(X, T) = -\frac{1}{2c_1} P_1 \left(T - \frac{X}{2c_1} \right) H \left(T - \frac{X}{2c_1} \right). \tag{4.14b}$$

Equations (4.6), (4.10), (4.13) and (4.14), combined with (4.1) and (4.2), determine the downstream flow completely. While these results have been derived assuming a mode-1 nonlinear wave, the main conclusions are still valid when the nonlinear wave is of mode $n > 1$. In this case, multiple shelves comprising linear long waves of mode $n, 2n, 3n, \dots$ are generated and, since $c_m \propto m^{-1}$, all these waves appear exclusively on the downstream side of the nonlinear wave. We also remark that the discontinuous behaviour at $X = c_m^\pm T$ of the shelves described by (4.10) and (4.14) indicates that dispersive effects are significant there and will act to smooth out the discontinuity, as demonstrated by Kodama & Ablowitz (1981) in the analogous problem of the perturbed KdV equation.

5. Mass conservation

We now verify that the downstream flow discussed above is consistent with mass conservation in the entire flow field.

Using (4.2) expression (3.6) for the net mass flux out of the main disturbance may be written as

$$\frac{dM}{dT} = -2\beta \sum_{n=0}^{\infty} \frac{P_{2n+1}}{(2n+1)\pi}. \tag{5.1}$$

On the other hand, from (4.6b) and (4.10b), the excess mass $M_m(T)$ in the shelf of

mode $m > 1$ is given by

$$M_m(T) = \beta(1 - \cos m\pi) \left[\int_0^{c_m^+ T} dX Q_m^+(\xi_m^+) - \int_0^{c_m^- T} dX Q_m^-(\xi_m^-) \right];$$

hence, upon differentiating with respect to T , the rate of change of mass within the mode- m shelf is

$$\frac{dM_m}{dT} = \beta(1 - \cos m\pi) \{c_m^+ Q_m^+(T) - c_m^- Q_m^-(T)\} \quad (m > 1). \quad (5.2a)$$

Likewise, using (4.14b), the rate of change of mass contained in the mode-1 shelf is found to be

$$\frac{dM_1}{dT} = -2\beta c_1 P_1(T). \quad (5.2b)$$

The rate of change of the total mass of the outer flow is then calculated by summing the expressions in (5.2a, b) over m :

$$\frac{dM}{dT} = -2\beta c_1 P_1(T) + 2\beta \sum_{n=1}^{\infty} \{c_{2n+1}^+ Q_{2n+1}^+(T) - c_{2n+1}^- Q_{2n+1}^-(T)\}. \quad (5.3)$$

Making use of (4.11), however, (5.3) reduces to

$$\frac{dM}{dT} = -2\beta \sum_{n=0}^{\infty} \frac{P_{2n+1}}{\pi(2n+1)},$$

which is precisely the mass flux out of the main nonlinear disturbance in (5.1). Therefore, the mass that leaves the nonlinear wave balances exactly that required to create the shelves downstream.

From the analysis of the outer flow in §4, it is clear that the downstream disturbance, even though it has $O(\mu^2)$ amplitude, carries $O(1)$ mass as it extends to $x = O(\mu^{-2})$ at $T = O(1)$. On the other hand, since the energy density is proportional to the square of the wave amplitude, the energy content of the shelves is $O(\mu^2)$ and energy, unlike mass, is conserved to leading order.

These results bear on the recent work of Prasad, Ramirez & Akylas (1996) who studied the generation of internal-wave disturbances by uniformly stratified Boussinesq flow of infinite depth over finite-amplitude topography. In this flow configuration following a similar matching procedure, it can be shown that shelves of small amplitude also appear downstream. Owing to the absence of a physical upper boundary, however, it turns out that the mass flux out of the main disturbance vanishes to leading order, so both the mass and the energy of the nonlinear wave are conserved (Prasad 1997). In fact, energy conservation proves helpful in interpreting the modulational instability of finite-amplitude steady-flow states, as discussed in Prasad *et al.* (1996).

6. Comparison with numerical results

It would be valuable to have confirmation of the predictions of the asymptotic theory from numerical simulations of nonlinear internal waves. For this purpose, we now examine shelf formation in a slightly different context where comparison with prior numerical work is feasible, at least qualitatively.

Specifically, we shall consider internal waves generated under resonance conditions by uniformly stratified Boussinesq flow of finite depth past bottom topography. Resonance occurs when the speed of the background flow V is close to one of the linear long-wave speeds c_n ($n = 1, 2, \dots$),

$$V = c_n(1 + \mu^2\lambda), \quad \lambda = O(1),$$

in which case a nonlinear mode- n wave disturbance of $O(1)$ amplitude is induced by small-amplitude topography, as explained in GY. The long-wave parameter $\mu \ll 1$ is now defined as h/W , where W is the characteristic width of the obstacle, and the shape of the obstacle is given by $y = \epsilon f(x)$, $\epsilon \ll 1$ being the ratio of the peak obstacle amplitude to the fluid depth h .

Following the procedure outlined in §2, taking $\epsilon = \mu^2$, the wave-amplitude profile of the resonant mode is governed by the forced analogue of the evolution equation (2.16):

$$K(x, x)A_T + \int_{-\infty}^x dx' K_x A'_T + \lambda c_n A_x - \frac{1}{2} c_n^3 A_{xxx} + c_n [(c_n^2 + A)f]_x = 0. \quad (6.1)$$

Observing that the formulation of GY was based on the vertical particle displacement rather than the streamfunction used in §2, the evolution equation (6.1) reduces to (4.3) of GY (in the special case of a uniform Boussinesq stratification) upon replacing A with $-A/c_n$ and appropriately rescaling T , f and λ .

Numerical solutions of (6.1) reveal the existence of a finite range of the resonance-detuning parameter λ over which a steady state is not reached; rather, the flow continues to evolve until wave breaking occurs and the formulation leading to (6.1) ceases to be valid. Based on our earlier finding that flow transience results in the generation of downstream shelves, without repeating the analysis of §4, it follows that the far wake of the obstacle is composed of all harmonics $m = pn$ ($p = 1, 2, \dots$) of the resonant mode n , forming multiple shelves of $O(\mu^2)$ amplitude. Furthermore, one expects the two fronts associated with the mode- m shelves to propagate downstream with speeds $V \pm c_m$.

The forced generation of internal waves in a uniformly stratified Boussinesq fluid layer has also been the focus of recent numerical investigations based on the full Navier–Stokes equations (Hanazaki 1992, 1993) or the inviscid equations of motion (Lamb 1994; Rottman, Broutman & Grimshaw 1996). With the exception of Lamb (1994), however, only the resonant-mode response is presented in these studies, precluding comparison with the multiple-shelf structure predicted by the asymptotic theory. The downstream boundary of the computational domain also was placed fairly close to the obstacle so the shelf of the resonant mode, which possesses the fastest travelling front, would exit the computational domain very rapidly. In addition, it is likely that the sponge layer used at the downstream boundary in the simulations of Rottman *et al.* (1996) would act to dissipate this shelf.

For these reasons, it was decided to concentrate on the simulations discussed by Lamb (1994) for the algebraic mountain (Witch of Agnesi), in particular the case described in terms of his amplitude and width parameters by $a = 0.13, D = 0.17$. The upstream conditions are such that $V = 0.826c_1$, implying a flow close to a mode-1 resonance. Switching to the dimensionless variables defined here, these flow conditions correspond to $\epsilon = \mu^2 = 0.13$ so $\lambda = -1.34$ and the obstacle profile in (6.1) is given by

$$f = \frac{1}{1 + 267x^2}. \quad (6.2)$$

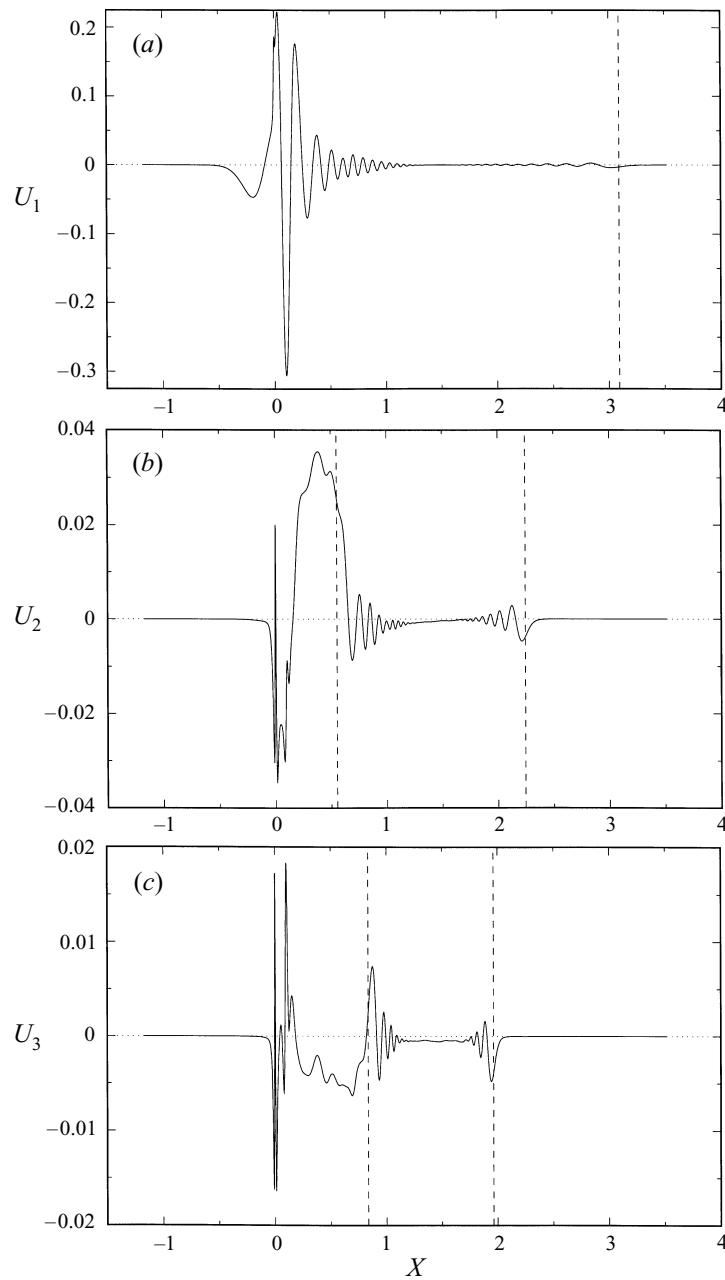


FIGURE 1. The results of the numerical simulations of Lamb (1994) at $T = 5.3$, showing the (a) mode-1, (b) mode-2 and (c) mode-3 waves. The theoretical locations of the shelf fronts are designated by the broken lines.

In presenting his results, Lamb (1994) employs a modal decomposition of the streamwise velocity which far downstream reduces to

$$u = V + \sum_{m=1}^{\infty} U_m \cos m\pi y. \quad (6.3)$$

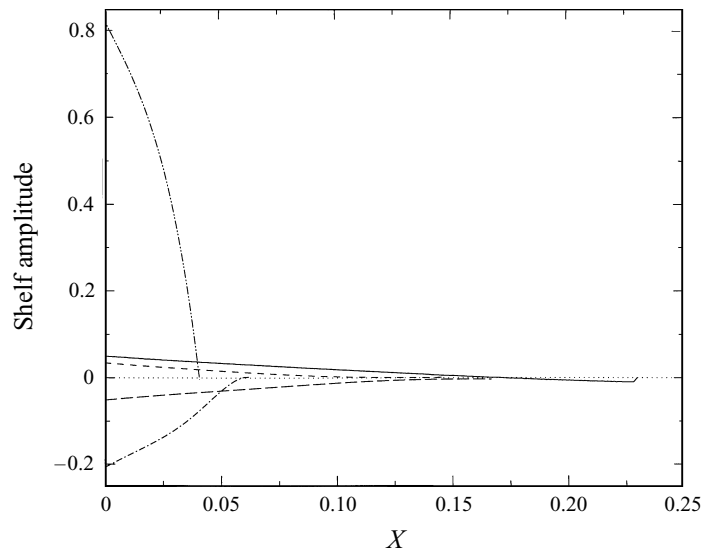


FIGURE 2. Shelf structure corresponding to the first three modes at the onset of wave breaking ($T = 0.4$), as predicted by the asymptotic theory. The lines represent respectively U_1 (—), U_2^+ (---), U_2^- (- · · -), U_3^+ (· · · ·) and U_3^- (- · · - ·). The abscissa is the outer coordinate $X = \mu^2 x$.

The spatial and temporal developments of the modal amplitudes U_1 and U_2 are illustrated in figure 9 of Lamb (1994). These amplitudes as well as the mode-3 response U_3 , which has been kindly provided to us by Dr Lamb, are plotted in figure 1 in terms of the outer coordinate X at $T = 5.3$ (corresponding to his $t = 30$). The obstacle is centred at $X = 0$ and has a streamwise extent $-0.1 \lesssim X \lesssim 0.1$. Furthermore, since V is known, the speeds of the shelf fronts are readily obtained, and the positions of these fronts at $T = 5.3$ are denoted in figure 1 by the broken lines. The mode-1 response U_1 in figure 1(a), consists of a large-amplitude wave above the obstacle, followed by a train of decaying lee waves. In addition, a small-amplitude disturbance is observed to form well beyond the lee wavetrain, at a position close to that of the mode-1 shelf. Turning now to figure 1(b,c), it is evident that U_2 and U_3 are each composed of two more or less separate disturbances that extend roughly to the positions of the shelf fronts Q_m^+ and Q_m^- ($m = 2, 3$) predicted by the asymptotic theory. While one might attribute the far-field disturbances in figure 1 to linear transients that are generated by the nearly impulsive startup of the flow, this interpretation is not supported by the sustained generation of higher-mode waves seen in figure 1(b,c) and in figure 9(d,f) of Lamb (1994), reinforcing the view that the observed far-field disturbances are actually shelves.

In an attempt to make a more detailed comparison between the asymptotic and numerical results, we next use the asymptotic theory to determine the response under the flow conditions considered in Lamb (1994) by numerically solving (6.1) subject to the forcing (6.2) for $n = 1$ and $\lambda = -1.34$. Wave breaking is found to occur at $T = 0.4$, which compares poorly with the value of $T \approx 5$ reported in Lamb (1994). This is not surprising since the forcing (6.2) is quite narrow so dispersive effects are not properly accounted for by the asymptotic theory. Consequently, the errors in estimating the shelf amplitudes are expected to be significant and comparison with the data of Lamb (1994) can only be qualitative, at best. From the known evolution of the resonant-wave amplitude, the structure of the shelves is then determined following

the methodology of §4. To facilitate comparison with Lamb (1994), the shelves are expressed in terms of the streamwise velocity rather than the streamfunction; with the notation of (6.3), we find from (4.3), (4.6a) and (4.10a) that

$$U_1 = \mu^2 \pi Q_1, \quad U_m = U_m^- H(T - X/c_m^-) + U_m^+ H(T - X/c_m^+) \quad (m \geq 2),$$

where

$$U_m^\pm = \mu^2 m \pi Q_m^\pm \quad (m \geq 2).$$

In particular, the amplitudes U_1 , U_2^\pm and U_3^\pm of the shelves corresponding to the first three modes are depicted in figure 2 at the onset of breaking. Despite the order-of-magnitude difference between the predicted values in figure 2 and the computed amplitudes in figure 1, certain qualitative similarities are apparent. Specifically, we observe that in both cases the ‘fast’ shelf components U_m^+ are significantly smaller in magnitude than their ‘slow’ counterparts U_m^- , and the slowest of all shelves, U_2^- , appears to be the dominant one. As pointed out earlier, the large error in estimating the shelf amplitudes is attributed to the fact that the obstacle profile (6.2) is far from hydrostatic; the agreement is likely to improve when a wider forcing is used, as assumed in the asymptotic theory.

7. Weakly nonlinear–weakly dispersive régime

The generation of shelves by finite-amplitude internal waves so far has been analysed in the context of a uniformly stratified Boussinesq fluid, when the nonlinear theory of GY is valid. It is natural, therefore, to ask whether similar phenomena can occur under more general flow conditions. Here we take up this question and consider internal waves in a fluid layer with arbitrary (stable) stratification. While no finite-amplitude theory is available in this setting, it will be shown based on the expansion procedure of Benney (1966) that the transient evolution of wave disturbances in the weakly nonlinear–weakly dispersive régime is indeed accompanied by shelves which, in general, appear both upstream and downstream.

To this end, returning to the formulation of §2, we now consider a mode- n long-wave disturbance of small amplitude $\epsilon \ll 1$, propagating from right to left along a fluid layer with general stratification. Adopting a reference frame translating with the corresponding linear long-wave speed $-c_n$, it is convenient to write

$$\Psi = c_n y + \epsilon \psi, \quad \rho = \bar{\rho}(y) + \epsilon q, \quad (7.1)$$

and work with ψ and q , the streamfunction and density perturbations, respectively. Assuming the traditional KdV balance $\epsilon = \mu^2$, the disturbance then evolves on the slow timescale $T = \epsilon t$, and the governing equations (2.2) and (2.3) take the form

$$c_n q_x - \bar{\rho}_y \psi_x = \epsilon [J(\psi, q) - q_T], \quad (7.2)$$

$$\begin{aligned} c_n (\bar{\rho} \psi_{yx})_y - \frac{q_x}{\beta} = & -\epsilon \left\{ c_n \bar{\rho} \psi_{xxx} + (\bar{\rho} \psi_{yT})_y + [\bar{\rho} J(\psi_y, \psi) + c_n q \psi_{yx}]_y \right\} \\ & - \epsilon^2 \left\{ [q J(\psi_y, \psi) + q \psi_{yT}]_y + c_n q \psi_{xxx} + [\bar{\rho} J(\psi_x, \psi)]_x \right\} \\ & + \epsilon^3 [q J(\psi, \psi_x)]_x. \end{aligned} \quad (7.3)$$

In addition, the boundary conditions (2.4) become

$$\psi_x = 0 \quad (y = 0, 1). \quad (7.4)$$

Following Benney (1966), we now expand

$$\psi = \psi^{(0)} + \epsilon\psi^{(1)} + \epsilon^2\psi^{(2)} + \dots, \tag{7.5a}$$

$$q = q^{(0)} + \epsilon q^{(1)} + \epsilon^2 q^{(2)} + \dots, \tag{7.5b}$$

the leading-order solution corresponding to a long wave of mode n as defined by (2.7) and (2.8):

$$\psi^{(0)} = a\phi_n(y), \quad q^{(0)} = \frac{a}{c_n} \bar{\rho}_y \phi_n(y). \tag{7.5c}$$

Furthermore, the amplitude $a(x, T)$ is constrained to satisfy an evolution equation of the form

$$\begin{aligned} a_T = & 2raa_x + sa_{xxx} + \epsilon [\alpha_1(a^3)_x + \alpha_2aa_{xxx} + \alpha_3a_xa_{xx} + \alpha_4a_{xxxx}] \\ & + \epsilon^2 [\gamma_1(a^4)_x + \gamma_2a^2a_{xxx} + \gamma_3aa_xa_{xx} + \gamma_4a_x^3 + \gamma_5aa_{xxxx} \\ & + \gamma_6a_xa_{xxxx} + \gamma_7a_{xx}a_{xxx} + \gamma_8a_{xxxxxx}] + O(\epsilon^3). \end{aligned} \tag{7.6}$$

To determine the constants $r, s, \alpha_1, \dots, \alpha_4$ and $\gamma_1, \dots, \gamma_8$, it is necessary to solve for the higher-order corrections $\psi^{(1)}, q^{(1)}$, etc. in (7.5), as explained in Benney (1996).

For our purposes, it is important to note that solutions of equation (7.6), like those of the integral-differential evolution equation (2.16) discussed earlier, remain locally confined. This indicates that the appearance of shelves, if any, must be reflected in the higher-order corrections to $\psi^{(0)}$ and $q^{(0)}$ in (7.5). In fact, as it turns out, one has to carry the perturbation theory to $O(\epsilon^3)$ in order to detect the presence of shelves, and, to avoid heavy algebraic manipulations, here we shall only sketch the main steps in the analysis (see Prasad 1997 for further details).

Briefly, it follows from (7.2)–(7.5) that the $O(\epsilon)$ corrections $\psi^{(1)}$ and $q^{(1)}$ take the separable form

$$\psi^{(1)} = a^2\phi^{(1,0)} + a_{xx}\phi^{(0,1)}, \tag{7.7a}$$

$$q^{(1)} = a^2q^{(1,0)} + a_{xx}q^{(0,1)}, \tag{7.7b}$$

where

$$q^{(1,0)} = \frac{\bar{\rho}_y}{c_n} \phi^{(1,0)} + \frac{1}{2c_n^2} \bar{\rho}_{yy} \phi_n^2 - \frac{r}{c_n^2} \bar{\rho}_y \phi_n, \tag{7.7c}$$

$$q^{(0,1)} = \frac{\bar{\rho}_y}{c_n} \phi^{(0,1)} - \frac{s}{c_n^2} \bar{\rho}_y \phi_n, \tag{7.7d}$$

and $\phi^{(1,0)}(y), \phi^{(0,1)}(y)$ satisfy certain inhomogeneous boundary-value problems (Benney 1966). Imposing solvability conditions on these problems determines the constants r and s :

$$r = -\frac{3}{4I} \int_0^1 dy \bar{\rho} \phi_{ny}^3, \quad s = \frac{c_n}{2I} \int_0^1 dy \bar{\rho} \phi_n^2, \tag{7.8}$$

where $I = \int_0^1 dy \bar{\rho} \phi_{ny}^2$.

Proceeding to $O(\epsilon^2)$, we write

$$\psi^{(2)} = a^3\phi^{(2,0)} + aa_{xx}\phi_1^{(1,1)} + a_x^2\phi_2^{(1,1)} + a_{xxxx}\phi^{(0,2)}, \tag{7.9a}$$

$$q^{(2)} = a^3q^{(2,0)} + aa_{xx}q_1^{(1,1)} + a_x^2q_2^{(1,1)} + a_{xxxx}q^{(0,2)}, \tag{7.9b}$$

where $q^{(2,0)}, \dots, q^{(0,2)}$ can be expressed in terms of $\phi^{(2,0)}, \dots, \phi^{(0,2)}$ and the known lower-order solutions. As before, $\phi^{(2,0)}(y), \dots, \phi^{(0,2)}(y)$ satisfy certain inhomogeneous

boundary-value problems, the solvability conditions of which specify the four constants $\alpha_1, \dots, \alpha_4$.

Thus far, there is no indication of shelf formation since ψ and q remain locally confined to $O(\epsilon^2)$ according to (7.7) and (7.9). Returning to (7.2), however, and integrating over x , we find upon using (7.6), (7.7) and (7.9) that

$$c_n q - \bar{\rho}_y \psi \Big|_{-\infty}^{\infty} = \epsilon^3 P \int_{-\infty}^{\infty} dx a_x^3 + O(\epsilon^4), \tag{7.10}$$

where

$$P(y) = \left[\phi_n \left(q_2^{(1,1)} - \frac{1}{2} q_1^{(1,1)} \right) + \phi^{(0,1)} q^{(1,0)} - \phi^{(1,0)} q^{(0,1)} \right]_y - \frac{1}{c_n} (\gamma_2 - \frac{1}{2} \gamma_3 + \gamma_4) \bar{\rho}_y \phi_n + \frac{1}{c_n} \bar{\rho}_y \left[\phi_n \left(\frac{1}{2} \phi_1^{(1,1)} - \phi_2^{(1,1)} \right) \right]_y - 3sq^{(2,0)} - 2r \left(q_2^{(1,1)} - q_1^{(1,1)} \right). \tag{7.11}$$

Equation (7.10) reveals the presence of shelves since the integral on the right-hand side is not zero in general. Using (7.1), (7.6) and with the rescaling $A = \epsilon a$, (7.10) can in fact be brought to a form analogous to (3.5):

$$c_n(\rho - \bar{\rho}) - \bar{\rho}_y \Psi \Big|_{-\infty}^{\infty} = \frac{\epsilon P}{3s} \frac{d}{dT} \int_{-\infty}^{\infty} dx A^3, \tag{7.12}$$

from which it is clear that shelves appear only when the flow is transient and are generated by nonlinear self-interaction of the main wave disturbance, the same mechanism as in a uniformly stratified Boussinesq fluid. In contrast to (3.5), however, one expects, in general, the vertical structure $P(y)$ in (7.11) to contain contributions from all long-wave modes $\phi_m(y)$ ($m = 1, 2, \dots$). This implies that the shelves associated with modes having speed $c_m > c_n$ would propagate both upstream (since $c_m^- = c_n - c_m < 0$) and downstream (since $c_m^+ = c_n + c_m > 0$), while those shelves corresponding to modes with speed $c_m < c_n$ (for which $c_m^\pm > 0$) would only appear downstream of the main wave.

Obtaining further information about the structure of shelves requires numerical solution of the boundary-value problems governing the $O(\epsilon)$ and $O(\epsilon^2)$ flow corrections in (7.7) and (7.9). In the special case of a uniformly stratified Boussinesq fluid, $\bar{\rho}_y = -\beta$, however, these problems can be solved in closed form, and it is easy to check that the results of the present formulation are consistent with those obtained earlier in the small-amplitude limit.

Specifically, from (2.9), $\phi_n = \sin n\pi y$ so $r = 0$ and $s = \frac{1}{2}c_n^3$ according to (7.8). At $O(\epsilon)$ then $\phi^{(1,0)} = \phi^{(0,1)} = 0$ so, from (7.7c, d), $q^{(1,0)} = 0$, $q^{(0,1)} = \frac{1}{2}\beta c_n \sin n\pi y$. Solvability conditions at $O(\epsilon^2)$ yield $\alpha_1 = \alpha_2 = \alpha_3 = 0$, $\alpha_4 = \frac{1}{8}c_n^4$, with the result that

$$\phi^{(2,0)} = 0, \quad \phi_1^{(1,1)} = \frac{1}{4} \sin 2n\pi y, \quad \phi_2^{(1,1)} = -\frac{1}{4} \sin 2n\pi y, \tag{7.13a}$$

and

$$q^{(2,0)} = 0, \quad q_1^{(1,1)} = -\frac{\beta}{2c_n} \sin 2n\pi y, \quad q_2^{(1,1)} = \frac{\beta}{2c_n} \sin 2n\pi y. \tag{7.13b}$$

Proceeding then to $O(\epsilon^3)$, it is readily shown that $\gamma_1 = \gamma_5 = \gamma_6 = \gamma_7 = 0$ and

$$\gamma_2 = \gamma_3 = -\frac{1}{4c_n}, \quad \gamma_4 = \frac{1}{2c_n}, \quad \gamma_8 = -\frac{c_n^8}{32}. \tag{7.14}$$

The evolution equation (7.6) hence reduces to

$$a_T - \frac{1}{2} c_n^3 a_{xxx} - \frac{1}{8} \epsilon c_n^4 a_{xxxxx} + \frac{\epsilon^2}{4c_n} a^2 a_{xxx} + \frac{\epsilon^2}{4c_n} a a_x a_{xx} - \frac{\epsilon^2}{2c_n} (a_x)^3 + \frac{1}{32} \epsilon^2 c_n^8 a_{xxxxxxx} = 0,$$

which, upon rescaling $A = \epsilon a$, agrees with (2.20), except for the higher-order dispersive terms. This discrepancy is not surprising because the theory of GY only accounts for the leading effects of dispersion.

Finally, inserting (7.13) and (7.14) into (7.11), (7.12) becomes

$$c_n(\rho - \bar{\rho}) + \beta \Psi \Big|_{-\infty}^{\infty} = \frac{\epsilon \beta}{8c_n^5} (\sin n\pi y + 3 \sin 3n\pi y) \frac{d}{dT} \int_{-\infty}^{\infty} dx A^3,$$

in agreement with (3.5). Of course, the lower limit of the left-hand side in the above expression vanishes because, as noted in §4, no shelves can propagate upstream in the case of a uniform Boussinesq stratification which, in this regard, is exceptional.

8. Discussion

The present investigation has addressed the problem of shelf formation in the context of internal waves in stratified flows. For fully nonlinear long waves in a uniformly stratified fluid of finite depth, it was pointed out that a downstream shelf of small amplitude exists when the flow is unsteady, which renders the nonlinear theory of GY invalid far downstream and causes a net efflux of mass. While this was not accounted for by GY, it does not alter the results obtained therein, which pertain to the near-field response. The downstream flow must be treated separately since the scales of the nonlinear theory no longer apply. Using a matching procedure, the downstream disturbance is found to consist of pairs of linear modes propagating at their linear long-wave speeds, and mass conservation is verified.

Physically, the presence of shelves in the downstream flow implies the existence of columnar disturbances with a high degree of spatial and temporal persistence. To the extent that the theory of GY may be regarded as a prototype for other finite-amplitude long-wave systems, one may also expect shelves to accompany transient nonlinear disturbances in a fluid layer with arbitrary stratification. In fact, our analysis in the weakly nonlinear–weakly dispersive régime indicates that shelves of fourth order in amplitude are formed. Moreover, these shelves contain components that propagate upstream of the main wave, revealing a type of upstream influence that has not been previously considered.

The question of upstream influence has been investigated theoretically by, among others, McIntyre (1972) in non-resonant uniformly stratified Boussinesq flow of finite depth over weakly nonlinear topography. By solving the transient problem using a perturbation expansion in terms of the topography amplitude parameter ϵ , McIntyre (1972) demonstrated that upstream-propagating disturbances of $O(\epsilon^2)$ may be generated by nonlinear interactions of the transient lee-wave ‘tails’. In contrast, the shelves discussed here have $O(\epsilon^4)$ amplitude in the weakly nonlinear–weakly dispersive régime, and are caused by transience of the main nonlinear long-wave disturbance. Parenthetically, we observe that in the case of a uniform Boussinesq stratification, considered by McIntyre (1972), no upstream shelves are predicted by the present theory.

Finally, we note that although the shelves discussed here are asymptotically small, they can be significant for narrow obstacles of finite amplitude, as illustrated by the simulations of Lamb (1994). In geophysical flows, these shelves would act to

enhance momentum transport, thereby increasing the drag force on the obstacle and altering, for example, the temperature distribution. In addition, their presence implies reduced towing times in tank experiments compared with values that might be anticipated based on linear theory, and bears on the implementation of suitable boundary conditions at the upstream and downstream edges of the computational domain in numerical simulations.

The authors wish to thank Dr Kevin G. Lamb for making available the results of his simulations shown in figure 1. This work was supported in part by the National Science Foundation Grant DMS-9404673 and the Air Force Office of Scientific Research Grant F49620-92-J-0086.

REFERENCES

- BENNEY, D. J. 1966 Long nonlinear waves in fluid flows. *J. Math. Phys.* **45**, 52–63.
- GRIMSHAW, R. & YI, X. 1991 Resonant generation of finite-amplitude waves by the flow of a uniformly stratified fluid over topography. *J. Fluid Mech.* **229**, 603–628 (referred to herein as GY).
- HANAZAKI, H. 1992 A numerical study of nonlinear waves in a transcritical flow of stratified fluid past an obstacle. *Phys. Fluids A* **4**, 2230–2243.
- HANAZAKI, H. 1993 On the nonlinear internal waves excited in the flow of a linearly stratified Boussinesq fluid. *Phys. Fluids A* **5**, 1201–1205.
- JOHNSON, R. S. 1973 On the development of a solitary wave moving over an uneven bottom. *Proc. Camb. Phil. Soc.* **73**, 183–203.
- KNICKERBOCKER, C. J. & NEWELL, A. C. 1980 Shelves and the Korteweg–de Vries equation. *J. Fluid Mech.* **98**, 803–818.
- KODAMA, Y. & ABLowitz, M. J. 1981 Perturbations of solitons and solitary waves. *Stud. Appl. Maths* **64**, 225–245.
- LAMB, K. G. 1994 Numerical simulations of stratified inviscid flow over a smooth obstacle. *J. Fluid Mech.* **260**, 1–22.
- LIEBOVICH, S. & RANDALL, J. D. 1973 Amplification and decay of long nonlinear waves. *J. Fluid Mech.* **58**, 481–493.
- LONG, R. R. 1953 Some aspects of the flow of stratified fluids. I. A theoretical investigation. *Tellus* **5**, 42–57.
- MCINTYRE, M. E. 1972 On Long's hypothesis of no upstream influence in uniformly stratified or rotating flow. *J. Fluid Mech.* **52**, 209–243.
- NEWELL, A. C. 1985 *Solitons in Mathematics and Physics*. SIAM.
- PRASAD, D. 1997 Dynamics of large-amplitude internal waves in stratified flows over topography. Doctoral dissertation, Department of Mechanical Engineering, MIT.
- PRASAD, D., RAMIREZ, J. & AKYLAS, T. R. 1996 Stability of stratified flow of large depth over finite-amplitude topography. *J. Fluid Mech.* **320**, 369–394.
- ROTTMAN, J. W., BROUTMAN, D. & GRIMSHAW, R. 1996 Numerical simulations of uniformly stratified fluid flow over topography. *J. Fluid Mech.* **306**, 1–30.
- WARN, T. 1983 The evolution of finite amplitude solitary Rossby waves on a weak shear. *Stud. Appl. Maths* **69**, 127–133.